BNL-108229-2015-JA

Itinerancy enhanced quantum fluctuation of magnetic moments in iron-based superconductors

Yu-Ting Tam (譚宇婷),[1,2] Dao-Xin Yao (姚道新),[1] and Wei Ku (顧威)[2,3,*]

[1]*State Key Laboratory of Optoelectronic Materials and Technologies, School of Physics and Engineering, Sun Yat-Sen University, Guangzhou 510275, China*

[2]*CMPMSD, Brookhaven National Laboratory, Upton, NY 11973-5000,U.S.A.*

[3]*Physics Department, State University of New York, Stony Brook, New York 11790, USA*

(Dated: July 22, 2015)

We investigate the influence of itinerant carriers on dynamics and fluctuation of local moments in Fe-based superconductors, via linear spin-wave analysis of a spin-fermion model containing both itinerant and local degrees of freedom. Surprisingly against the common lore, instead of enhancing the (π,0) order, itinerant carriers with well nested Fermi surfaces is found to induce significant amount of *spatial* and temporal quantum fluctuation that leads to the observed small ordered moment. Interestingly, the underlying mechanism is shown to be intra-pocket nesting-associated long-range coupling, rather than the previously believed ferromagnetic double-exchange effect. This challenges the validity of ferromagnetically compensated first-neighbor coupling reported from short-range fitting to the experimental dispersion, which turns out to result instead from the ferro-orbital order that is also found instrumental in stabilizing the magnetic order.

PACS numbers: 74.70.Xa, 74.20.Pq, 74.25.Ha, 75.30.-m

In the decades-long quest to understand high-temperature superconductivity, antiferromagnetic (AFM) correlation has been one of the primary research focuses, due to its frequent proximity to superconductivity in the phase diagram. The newly discovered Fe-based superconductors (Fe-SC) add another interesting example to such proximity: the parent compounds next to the superconducting phase possess a (π,0) C-type antiferromagnetic (C-AFM) correlation, antiferromagnetic along the x-direction and ferromagnetic along the y-direction. This C-AFM is further accompanied by a strong coupling to a ferro-orbital (FO) [1–3] (or nematic [4]) and structural correlation that breaks the lattice rotational symmetry and suppresses fluctuation to the (0,π) C-AFM correlation. Upon doping, the C-AFM correlation no longer condenses into a long-range order, but still persists at short range in the superconducting regime [5], suggesting its importance in the underlying electronic structure that hosts superconductivity.

Interestingly, even in the undoped parent compounds, the C-AFM order presents an unusual characteristic: the ordered magnetic moment is much smaller than the local moment. Indeed, Table I that summarizes the experimentally estimated moments at low temperature, shows a systematic large reduction of ordered moment from the local moment across all families of Fe-SC. That is, the local moment fluctuates strongly such that only about half of it remains ordered. Such a systematic, strong quantum fluctuation is obviously physically significant, but poses a serious challenge to the proper understanding of the magnetism. Currently, this fluctuation is attributed to strong temporal fluctuation from studies [6–8] employing dynamical mean-field approximation. However, it is unclear whether this picture is handicapped by the intrinsic limitation of such a mean-field approximation that does not allow spatial fluctuation.

TABLE I: Large difference in local and ordered moments.
† theoretical estimation in the lack of the experimental value

System	local moment(μ_B)	ordered moment(μ_B)
LaFeAsO	$1.1 \sim 2.4^\dagger$ [9]	0.36 [10]
CeFeAsO	1.3 [11]	0.8 [12]
PrFeAsO	1.3 [13]	0.53 [14]
FeTe	$2 \sim 3$ [15]	> 2 [16]
$BaFe_2As_2$	1.3 [13]	0.87[17]
$SrFe_2AS_2$	2.1 [11]	0.94 [18]

This issue is further complicated by the presence of both large local moments and the low-energy itinerant carriers in the system. Indeed, the Fermi surface was found [19, 20] to consist of electron and hole pockets that are approximately nested by $q = (\pi, 0)$. The presence of both itinerant carriers and local moments renders the knowledge obtained from pure local pictures (e.g. Heisenberg model) and the pure itinerant pictures (e.g. nesting of the Fermi surface) fundamentally inadequate. Recently, it was proposed [21] that the itinerant carriers introduces a strong *ferromagnetic* correlation along the y-direction (so-called double exchange effect) that stabilizes the C-AFM. Another study [22], however, attributed stability of C-AFM to the assistance of the *antiferromagnetic* nesting of the Fermi surface. Obviously, it is important and timely to clarify how the itinerant carriers modulate the dynamics and fluctuation of the local moments, and to reveal the dominant magnetic mechanism and the role of the Fermi surface nesting.

In this Letter, we investigate the influence of the itinerant carriers on the dynamics and fluctuation of the lo-

cal moments, using a spin-fermion model with ferromagnetic Hund's coupling. Surprisingly, upon integrating out the itinerant degree of freedom within a linear spin-wave analysis, we found that itinerant carriers with well nested Fermi surface, instead of enhancing the C-AFM order, actually induce large *spatial* and temporal quantum fluctuation that reduces the ordered moment significantly. Interesting, the itinerancy induced renormalization of long-range magnetic couplings gives a strong *antiferromagnetic* first-neighboring coupling that tends to destabilize the C-AFM order. This is opposite to the ferromagnetic double-exchange effect previously proposed [21] to explain the seemingly ferromagnetically compensated first-neighbor coupling [23] from short-range fitting of the experimental dispersion. Our result challenges the validity of such fitting, and demonstrates the true origin being the FO order instead, which is found also instrumental in stabilizing the C-AFM order. Our study not only explains the strong moment-fluctuation in Fe-SCs, but also advocates future investigations of itinerant-local interplay in strongly correlated materials.

The simplest model to describe systems consisting of local and itinerant degrees of freedom is the spin-fermion model [21, 24–26]:

$$\begin{aligned}\mathcal{H} &= J_1 \sum_{<i,i'>} \vec{S}_i \cdot \vec{S}_{i'} + J_2 \sum_{<<i,i'>>} \vec{S}_i \cdot \vec{S}_{i'} \\ &- J_H \sum_{i,m,ss'} \vec{S}_i \cdot c^\dagger_{ims} \vec{\sigma}_{ss'} c_{ims'} \\ &- \sum_{ii',mm',s} t^{mm'}_{ii'} c^\dagger_{ims} c_{i'm's} + \sum_{i,m,s} (\epsilon\eta_m - \mu) c^\dagger_{ims} c_{ims},\end{aligned} \tag{1}$$

in which the local moments S_i at site i couples antiferromagnetically to its first and second neighbors via J_1 and J_2, and couples ferromagnetically to the itinerant carriers via Hund's coupling J_H. (Here $\vec{\sigma}_{ss'}$ is the usual Pauli matrices.) The itinerant carrier $c^\dagger_{ims}$ of orbital m and spin s at site i hops with parameter $t_{ii'}$. Since Eq. 1 lacks interaction between fermions that drives the intrinsic orbital instability, we include the effect of FO order via an order parameter ϵ that shifts the yz/xz orbital upward/downward by η_m. The chemical potential μ is evaluated for each set of magnetic and orbital order parameters to ensures equal number of electron and hole carriers, corresponding to the undoped parent compounds.

Very often, this model is applied to incorporate only a subset of the bands of the five Fe d-bands as itinerant carriers, having in mind that the rest of the bands constitute the local moment [21, 24–26], consistent with the notion of orbital selective Mott transition [27]. However, such clean separation is not the only way in which the spin-fermion model can be justified or utilized. Generally speaking, the physics to be captured in the model is how the kinetic energy of the low-energy carriers interplay with the potential energy of local moments that are low-energy in the spin (particle-hole) channel but high-energy in the one-particle spectral function. In line with this spirit, we include all five low-energy Fe-As hybrid d-orbitals in order to capture the realistic Fermi surface, knowing that only the low-energy portion of the carriers will contribute to the renormalization of magnetic coupling between local moments. (Analogously, Hubbard's treatment of thermal fluctuation in itinerant magnetism for Fe and Ni [28, 29] also include the full itinerant bands, with S termed "exchange field".) Specifically, we obtain first a 10-band 3D Hamiltonian from density functional theory, represented by the low-energy Wannier function [30]. We then reduce it to a 5-band 2D Hamiltonian in the pseudo-momentum space via the local gauge transformation [31–33] and apply it to Eq. 1.

Since we are mostly interested in the generic *qualitative* trends how the itinerant carriers modify the dynamics and fluctuation of the local moments in all the FeSC families, we choose the prototypical LaOFeAs for the illustration below. We follow the procedure of Ref. [21] to integrate out the itinerant carriers up to the 2nd order in J_H/S within the linear spin-wave theory (assisted by Holstein-Primakoff transformation, as usual) [31] while fixing $S = 1$ as a representative case. A discrete 500x500 momentum mesh and a thermal broadening of 100meV are used to ensure a good convergence and to avoid material-specific features [34]. The resulting renormalized spin-wave Hamiltonian (in unit of S^2)

$$\mathcal{H}^{\mathcal{SW}} = \sum_q A_q (a^\dagger_q a_q + a_{-q} a^\dagger_{-q}) + B_q (a^\dagger_q a^\dagger_{-q} + a_{-q} a_q) \tag{2}$$

corresponds to a Heisenberg Hamiltonian of the local moments with renormalized long-range coupling $\tilde{J}_{ii'}$

$$\tilde{\mathcal{H}} = \sum_{i,i'} \tilde{J}_{ii'} S_i \cdot S_{i'}, \tag{3}$$

and gives the spin-wave dispersion and fluctuation of the ordered moment [31]. All the results below correspond to bare couplings of the local moment $J_1 = 19$meV and $J_2 = 13$meV that, after renormalization, give the correct experimental spin-wave bandwidth ($\sim$ 200meV [23, 35–37]) and a sufficiently stable C-AFM phase.

To visualize the overall effects of itinerant carriers, Fig. 1(a) shows the resulting renormalized spin-wave dispersion for a fixed strength of FO order. As the coupling J_H to itinerant carriers increases from 0.45eV to 0.64eV, the dispersion becomes stronger along the antiferromagnetic x-direction [(0,0)-(π,0)], while the ferromagnetic y-direction [(π,0)-(π,π)] is only weakly affected. This indicates that the dominant physical effect is *not* the ferromagnetic double exchange effect proposed previously [21], but instead an enhancement of the AFM couplings. This qualitative contrast in the physical conclusions is related to the employed fermion Fermi surface. Focusing on cases with low density ($\sim$ 0.1), Ref. [21] used only two small electron-pockets but no hole-pockets [31],

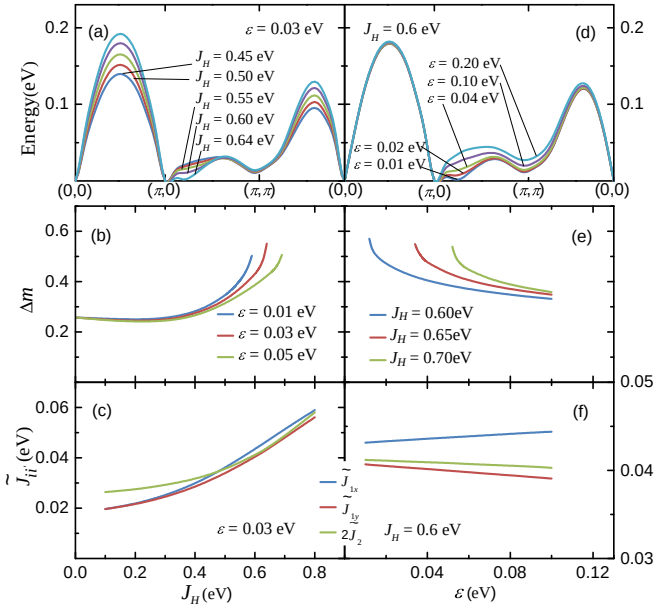

FIG. 1: (Color online) spin-wave dispersion ω_q along the high-symmetry paths (a) for a fixed FO order parameter ϵ and (d) for a fixed Hund's coupling J_H, (b)&(e) reduced ordered moment Δm for various J_H and ϵ, and renormalized first-neighbor couplings in x-direction $\tilde{J}_{1x}$, y-direction $\tilde{J}_{1y}$, and second neighbor coupling $\tilde{J}_2$ as functions of (c) J_H and (f) ϵ.

and thus favored nearly ferromagnetic couplings. On the other hand, our realistic Fermi surface has compensated hole- and electron-pockets separated by (π,0) and (0,π), which promotes AFM couplings at short range.

The induced AFM coupling turns out to fluctuate significantly the C-AFM state. Fig. 1(b) shows that as J_H increases beyond 0.4eV, the fluctuating portion of the moment [38]

$$\Delta m = 1/(8\pi^2)\int dq^2[1-(B_q/A_q)^2]^{-1/2} - 1/2 \qquad (4)$$

grows quickly and easily exceed 0.5, half of the local moment, accounting for the experimental observation. Since this quantum fluctuation originates from spontaneous creation of propagating magnons in a perfectly ordered state [39, 40], it is naturlaly *spatial* and temporal.

More detailed microscopic understanding of this AFM coupling-induced fluctuation can be obtained from Fig. 1(c) that shows the renormalized first-neighboring couplings in x- and y-directions ($\tilde{J}_{1x}$ and $\tilde{J}_{1y}$), and the renormalized second-neighboring coupling ($\tilde{J}_2$), for the case of ϵ = 30meV as an example. As J_H grows near 0.6eV, $\tilde{J}_{1y}$ increases faster than $2\tilde{J}_2$ and eventually approaches the latter, a situation in which the C-AFM state becomes unstable against (π,q)-fluctuation ($-\pi \le q \le \pi$) according to the simple classical energy estimation of the short-range J_1-J_2 model.

In other words, even though itinerant carriers themselves, having an approximate (π,0) nesting, prefer C-AFM correlation, their influence on the couplings of local moments, however, gives a larger $\tilde{J}_{1y}$ that disfavors the C-AFM correlation and produces strong fluctuation. Evidently, the previously reported itenerant nesting-enhanced susceptibility at (π,0) [22] is insufficient to conclude a more stabile C-AFM state. Instead, the even stronger enhancement of (π,q) fluctuation reveals the dominant role of itinerant carriers in reducing the C-AFM ordered moment. Such a surprising effect merely reflects the rich interplay between the itinerant carriers and local moments in our model, and set an alarming example against the usual itinerant-only considerations (e.g. the typical normal-state nesting arguments).

TABLE II: Importance of induced long-range couplings

J_H = 0.6 eV, ϵ = 0.03 eV	$q = (\pi, \frac{\pi}{5})$ full/up-to-$\tilde{J}_2$	$q = (\pi, \pi)$ full/up-to-$\tilde{J}_2$
A_q	0.1534/0.1558	0.0134/0.0316
B_q	-0.1527/-0.1532	0.0022/-0.0049
w_q	0.0103/0.0281	0.0132/0.0312

It is important to note the significant contributions of the RKKY-like long-range (power-law decaying) couplings between local moments induced by itinerant carriers [41]. Indeed, besides the leading $\tilde{J}_{1x}$, $\tilde{J}_{1y}$, and $\tilde{J}_2$, the resulting renormalized coupling $\tilde{J}$ contains small but long-range components that add up to important contributions. Table II gives an example of the calculated A_q, B_q and the spin-wave energy w_q, with and without the long-range couplings. It shows that inclusion of long-range couplings can change these values by a factor of two, confirming their importance. This is another alarming message to the common analysis of inelastic neutron scattering measurements that use only short-range couplings to fit the experimental data. For systems with itinerant carriers and consequently long-range magnetic couplings, such fitting can be dangerously misleading about the important physical effects.

The long range of the couplings naturally enables local moments to fluctuate with extended *spatial* structures. For example, the spin-wave dispersion in Fig. 1(a) shows a softening in the vicinity of (π,π/5), indicating strong fluctuation approximately in period of 10 unit cells. Our results therefore conclude a strong *spatial* fluctuation in addition to the currently emphasized temporal fluctuation [6–8] of the magnetic moment.

The origin of the enhanced fluctuation in the vicinity of (π,π/5) can actually be associated with the Fermi surface of the *ordered* state. As an illustration, Fig 2(a) shows the Fermi surface modified by the C-AFM and FO order parameters, unfolded in one-Fe Brillouin zone. One can observe an approximate intra-pocket nesting of (0, $2k_F$)$\sim$(0, π/5), equivalent to (π, π/5), matching the momentum region of the spin-wave softening and the enhanced fluctuation in Fig 2(b). In essence, the short-

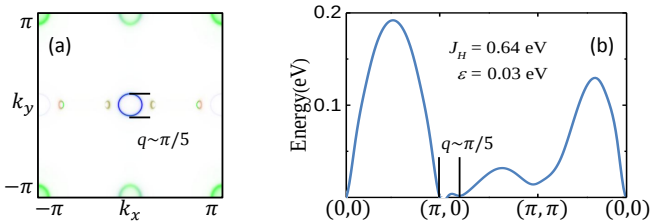

FIG. 2: (Color online) (a)Nesting of Fermi surface of a C-AFM and FO ordered state, unfolded in one-Fe Brillouin zone, and (b)its effect on the momentum region with spin-wave softening and enhanced fluctuation.

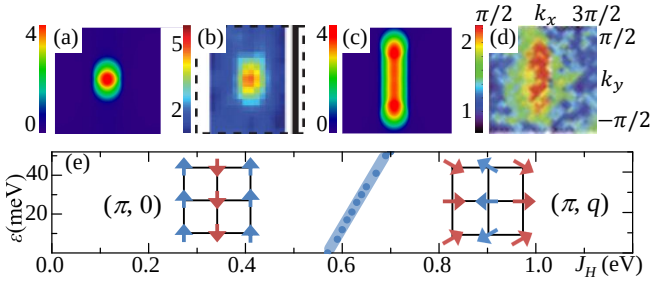

FIG. 3: (Color online) Theoretical momentum distribution of magnetic excitation at 10±1meV in (a) the C-AFM state (J_H=0.45eV,ϵ=30meV) and (c) a highly fluctuating state (J_H=0.64eV,ϵ=30meV), in 0.07π momentum-resolution. The latter shows enlongated (π,q) fluctuation, as measured in (d) spin-disordered $FeTe_{0.51}Se_{0.49}$ [42] when compared with (b) spin-ordered $BaFe_2As_2$ [49]. (e) Phase diagram showing the stable region of the C-AFM state.

range frustration of couplings enhances the overall spin fluctuation along (π,0) to (π,π), while the nesting of the Fermi surface of the *ordered* state pinpoints a more specific momentum region with most fluctuation.

Note that the "incommensurate" (π,q) excitation has in fact been observed in several materials [5, 42–44]. Figure 3(a)-(d) compare theoretical and experimental low-energy excitations of a C-AFM state and a strongly fluctuating state. The latter clearly has a more pronounced (π,q) momentum distribution, confirming their direct connection to the moment fluctuation.

Having established the main physical effects of the itinerant carriers, we now illustrate the essential role of the FO order in the C-AFM state using the right panels of Fig 1. Figure 1(d) shows clearly that a stronger FO order increases the dispersion along the path from (π,0) to (π,π), but barely changes the dispersion along the antiferromagnetic x-direction. In some of the Fe-SCs, such an enhanced spin-wave dispersion along the ferromagnetic y-direction has in fact been observed experimentally [23], and was previously attributed to a nearly compensated $\tilde{J}_{1y}$. This appears to suggest a large ferromagnetic double exchange effect. However, as discussed above, our realistic Fermi surface produces largely enhanced AFM $\tilde{J}_{1x}$, $\tilde{J}_{1y}$ and $\tilde{J}_2$, and thus does not support the double exchange picture. Indeed, Fig. 1(f) shows that this remains true even after introduction of the FO order: While $\tilde{J}_{1x}$ and $\tilde{J}_{1y}$ are slightly split by the anisotropy introduced by FO, they remain strongly antiferromagnetic.

Our results in Fig 1 thus uncovers the FO order being the true key physical effect. More microscopically, it is the FO order induced anisotropy in the renormalized coupling $\tilde{J}$ that raises the spin-wave energy along the path from (π,0) to (π,π) and slightly reduce the fluctuation. While the C-AFM order can also introduce the anisotropy, Fig. 1(a)(b) clearly indicates their different physical effects: C-AFM order enhances the dispersion along the x-direction, but FO order the y-direction. It is now also understandable why the experimental fitting may lead to nearly compensated $\tilde{J}_{1y}$: the fitting assigns all the anisotropy to one short-range coupling, even though in reality such anisotropy is spread out to a large number of long-range couplings instead, dictated by the itinerant nature.

In fact, the FO order is found essential to the C-AFM order. For example, in Fig. 1(f) $\tilde{J}_{1y} > 2\tilde{J}_2$ suggests that the C-AFM state should already be unstable if it weren't for the FO-induced anisotropy in the couplings. Indeed, one sees in Fig. 1(e) that a stronger FO order helps to reduce the moment fluctuation. Within the realistic parameter range, our result gives a phase diagram in Fig. 3, in which the C-AFM order requires the FO order for $J_H > 0.57$eV. This accounts naturally for the experimental fact across all Fe-SC families, that the FO/structural order always precedes the magnetic order [12, 45–47]. Of course, if the fluctuation in the extended (π,q) region overwhelms the aid from the FO order, the C-AFM order will still be destroyed. This gives the simplest explanation of the absence of magnetic order in FeSe, which still presents a strong FO/structural order [48]. Sure enough, spin-disordered Se-rich $FeTe_{1-x}Se_x$ [42–44] samples all present extended (π,q) fluctuation similar to Fig. 3(d).

In conclusion, we investigate the generic effects of itinerant carriers on the dynamics and fluctuation of local moments in the parent compounds of Fe-based superconductors, by integrating out the itinerant carriers that couple to the local moment via Hund's coupling. Unexpectedly, while the (π,0)-nested itinerant carriers alone prefers a C-AFM order, they however fluctuate efficiently C-AFM ordered local moments and produce the experimentally observed large reduction of the latter. Interestingly, the itinerant carriers induce long-range couplings between local moments with AFM first-neighboring couplings, producing strong *spatial* and temporal quantum fluctuation. This surprising finding is opposite to the common intuition of the nesting effect, and is distinct from the ferromagnetic double-exchange physics proposed previously to explain the seemingly ferromagnetic compensated first-neighbor coupling from short-range fitting of measured spin-wave dispersion. Our result challenges the validity of such fitting and demonstrates that

such dispersion results naturally from the FO order, which is also essential in stabilizing the C-AFM. These new insights illustrate the generic rich interplay between itinerant and localized degrees of freedom in many-body systems, and advocate further systematic investigation of transport, superconductivity, and other fluctuation dominant phenomena in these systems.

We thank Fan Yang and Hai-Qing Lin for helpful discussion, and Beijing Computational Science Center for its warm hospitality in hosting part of the research activity. WK acknowledges support from U.S. Department of Energy, Office of Basic Energy Science, Contract No. DE-AC02-98CH10886. YT and DXY acknowledge support from NBRPC-2012CB821400, NSFC-11275279, SRFDP-20110171110026,and NCET-11-0547.

* corresponding email: weiku@bnl.gov

[1] C.-C. Lee, W.-G. Yin, and W. Ku, Phys. Rev. Lett. **103**, 267001 (2009), URL http://link.aps.org/doi/10.1103/PhysRevLett.103.267001.

[2] F. Krüger, S. Kumar, J. Zaanen, and J. van den Brink, Phys. Rev. B **79**, 054504 (2009), URL http://link.aps.org/doi/10.1103/PhysRevB.79.054504.

[3] R. R. Singh, arXiv:0903.4408 (2009), URL http://http://arxiv.org/abs/0903.4408v1.

[4] J. R.M.Fernandes, A.V.Chubukov, Nature Physics **10**, 97 (2014).

[5] H. Luo, R. Zhang, M. Laver, Z. Yamani, M. Wang, X. Lu, M. Wang, Y. Chen, S. Li, S. Chang, et al., Phys. Rev. Lett. **108**, 247002 (2012), URL http://link.aps.org/doi/10.1103/PhysRevLett.108.247002.

[6] Z. P. Yin, K. Haule, and G. Kotliar, Nature Physics **7**, 294 (2011).

[7] P. Hansmann, R. Arita, A. Toschi, S. Sakai, G. Sangiovanni, and K. Held, Physical Review Letters **104**, 197002 (2010).

[8] Y.-Z. Zhang, H. Lee, I. Opahle, H. O. Jeschke, and V. Roser, Journal of Physics and Chemistry of Solids **72**, 324 (2011).

[9] Z. P. Yin, S. Lebegue, M. J. Han, B. P. Neal, S. Y. Savrasov, and W. E. Pickett, Physical Review Letters **101**, 047001 (2008).

[10] C. de la Cruz, Q. Huang, J. W. Lynn, J. Li, W. R. Ii, J. L. Zarestky, H. A. Mook, G. F. Chen, J. L. Luo, N. L. Wang, et al., Nature **453**, 899 (2008).

[11] P. Vilmercati, A. Fedorov, F. Bondino, F. Offi, G. Panaccione, P. Lacovig, L. Simonelli, M. A. McGuire, A. S. M. Sefat, D. Mandrus, et al., Physical Review B **85**, 220503 (2012).

[12] J. Zhao, Q. Huang, C. de la Cruz, S. Li, J. W. Lynn, Y. Chen, M. A. Green, G. F. Chen, G. Li, Z. Li, et al., Nature Materials **7**, 953 (2008).

[13] H. Gretarsson, A. Lupascu, J. Kim, D. Casa, T. Gog, W. Wu, S. R. Julian, Z. J. Xu, J. S. Wen, G. D. Gu, et al., Physical Review B **84**, 100509 (2011).

[14] S. Kimber, D. Argyriou, F. Yokaichiya, K. Habicht, S. Gerischer, T. Hansen, T. Chatterji, R. Klingeler, C. Hess, G. Behr, et al., Physical Review B **78**, 140503 (2008).

[15] I. A. Zaliznyak, Z. Xu, J. M. Tranquada, G. Gu, A. M. Tsvelik, and M. B. Stone, Physical Review Letters **107**, 216403 (2011).

[16] T. J. Liu, J. Hu, B. Qian, D. Fobes, Z. Q. Mao, W. Bao, M. Reehuis, S. A. J. Kimber, K. Proke, S. Matas, et al., Nature Materials **9**, 718 (2010).

[17] Q. Huang, Y. Qiu, W. Bao, M. A. Green, J. W. Lynn, Y. C. Gasparovic, T. Wu, G. Wu, and X. H. Chen, Physical Review Letters **101**, 257003 (2008).

[18] J. Zhao, W. Ratcliff, J. W. Lynn, G. F. Chen, J. L. Luo, N. L. Wang, J. Hu, and P. Dai, Physical Review B **78**, 140504 (2008).

[19] H. Ding, P. Richard, K. Nakayama, K. Sugawara, T. Arakane, Y. Sekiba, A. Takayama, S. Souma, T. Sato, T. Takahashi, et al., EuroPhysics Letters **83**, 47001 (2008).

[20] P. Richard, T. Sato, K. Nakayama, T. Takahashi, and H. Ding, Report on Progress in Physics **74**, 124512 (2011).

[21] W. Lv, F. Krüger, and P. Phillips, Phys. Rev. B **82**, 045125 (2010), URL http://link.aps.org/doi/10.1103/PhysRevB.82.045125.

[22] Y.-Z. You and Z.-Y. Weng, New Journal of Physics **16**, 023001 (2014).

[23] J. Zhao, D. T. Adroja, D.-X. Yao, R. Bewley, S. Li, X. F. Wang, G. Wu, X. H. Chen, J. Hu, and P. Dai, Nature Physics **5**, 555 (2009).

[24] W.-G. Yin, C.-C. Lee, and W. Ku, Phys. Rev. Lett. **105**, 107004 (2010), URL http://link.aps.org/doi/10.1103/PhysRevLett.105.107004.

[25] S.-P. Kou, T. Li, and Z.-Y. Weng, EPL (Europhysics Letters) **88**, 17010 (2009).

[26] S. Liang, G. Alvarez, C. Şen, A. Moreo, and E. Dagotto, Phys. Rev. Lett. **109**, 047001 (2012), URL http://link.aps.org/doi/10.1103/PhysRevLett.109.047001.

[27] L. de'Medici, G. Giovannetti, and M. Capone, Phys. Rev. Lett. **112**, 177001 (2014), URL http://link.aps.org/doi/10.1103/PhysRevLett.112.177001.

[28] J. Hubbard, Phys. Rev. B **20**, 4584 (1979), URL http://link.aps.org/doi/10.1103/PhysRevB.20.4584.

[29] J. Hubbard, Phys. Rev. B **23**, 5974 (1981), URL http://link.aps.org/doi/10.1103/PhysRevB.23.5974.

[30] W. Ku, H. Rosner, W. E. Pickett, and R. T. Scalettar, Phys. Rev. Lett. **89**, 167204 (2002), URL http://link.aps.org/doi/10.1103/PhysRevLett.89.167204.

[31] *Supplementary material.*

[32] C.-H. Lin, C.-P. Chou, W.-G. Yin, and W. Ku, arXiv **:1403.3687** (2014).

[33] P. A. Lee and X.-G. Wen, Phys. Rev. B **78**, 144517 (2008), URL http://link.aps.org/doi/10.1103/PhysRevB.78.144517.

[34] *The 0.1ev broadening is small enough compared to the electron band width, but large enough to sample well the gerentic features of the electron and hole pockets in all the fe-scs. as shown in [31] using a smaller broadening gives identicial trends, but may start to result in high sensitivity to the details of the fermi surface and thus materials dependent features undesired for our study.*

[35] L. W. Harriger, M. Liu, H. Luo, R. A. Ewings, C. D. Frost, T. G. Perring, and P. Dai, Physical Review B **86**, 140403 (2012).

[36] M. Ramazanoglu, J. Lamsal, G. S. Tucker, J. Q. Yan, S. Calder, T. Guidi, T. Perring, R. W. McCallum, T. A.

Lograsso, A. Kreyssig, et al., Physical Review B **87**, 140509 (2013).

[37] M. Wang, X. C. Wang, D. L. Abernathy, L. W. Harriger, H. Q. Luo, Y. Zhao, J. W. Lynn, Q. Q. Liu, C. Q. Jin, C. Fang, et al., Physical Review B **83**, 220515(R) (2011).

[38] D.-X. Yao and E. W. Carlson, Physical Review B **78**, 052507 (2008).

[39] R. Kubo, Phys. Rev. **87**, 568 (1952), URL `http://link.aps.org/doi/10.1103/PhysRev.87.568`.

[40] A. Auerbach, *Interacting Electrons and Quantum Magnetism* (Springer New York, 2012), chap. 11.

[41] *This long-range renormalization of coupings between local moments is to be distinquished from the long-range magnetic couplings among itinerant carriers discussed previously, for example in i. i. mazin et. al., phys. rev. b 78, 085104 (2008).*

[42] M. D. Lumsden, A. D. Christianson, E. A. Goremychkin, S. E. Nagler, H. A. Mook, M. B. Stone, D. L. Abernathy, T. Guidi, G. J. MacDougall, C. de la Cruz, et al., Nat. Phys. **6**, 182 (2010).

[43] D. N. Argyriou, A. Hiess, A. Akbari, I. Eremin, M. M. Korshunov, J. Hu, B. Qian, Z. Mao, Y. Qiu, C. Broholm, et al., Phys. Rev. B **81**, 220503 (2010).

[44] I. A. Zaliznyak, A. T. Savici, M. Lumsden, A. M. Tsvelik, R. Hu, and C. Petrovic, arXiv:1502.06051 (2015).

[45] C. R. Rotundu, D. T. Keane, B. Freelon, S. D. Wilson, A. Kim, P. N. Valdivia, E. Bourret-Courchesne, and R. J. Birgeneau, Phys. Rev. B **80**, 144517 (2009).

[46] N. Ni, M. E. Tillman, J.-Q. Yan, A. Kracher, S. T. Hannahs, S. L. Bud'ko, and P. C. Canfield, Phys. Rev. B **78**, 214515 (2008).

[47] S. Kasahara, T. Shibauchi, K. Hashimoto, K. Ikada, S. Tonegawa, R. Okazaki, H. Shishido, H. Ikeda, H. Takeya, K. Hirata, et al., Phys. Rev. B **81**, 184519 (2010).

[48] S. Medvedev, T. M. McQueen, I. A. Troyan, T. Palasyuk, M. I. Eremets, R. J. Cava, S. Naghavi, F. Casper, V. Ksenofontov, G. Wortmann, et al., Nat Mater **8**, 630 (2009).

[49] L. W. Harriger, H. Q. Luo, M. S. Liu, C. Frost, J. P. Hu, M. R. Norman, and P. Dai, Phys. Rev. B **84**, 054544 (2011), URL `http://link.aps.org/doi/10.1103/PhysRevB.84.054544`.

Supplementary

This supplementary provides additional detailed information about our calculation that is based on well-established methods in the literature.

I. Preparing for the 5-band Hamiltonian of the itinerant carriers

The figure below illustrates the overall computation scheme already outlined in the manuscript, involving several well-established methods.

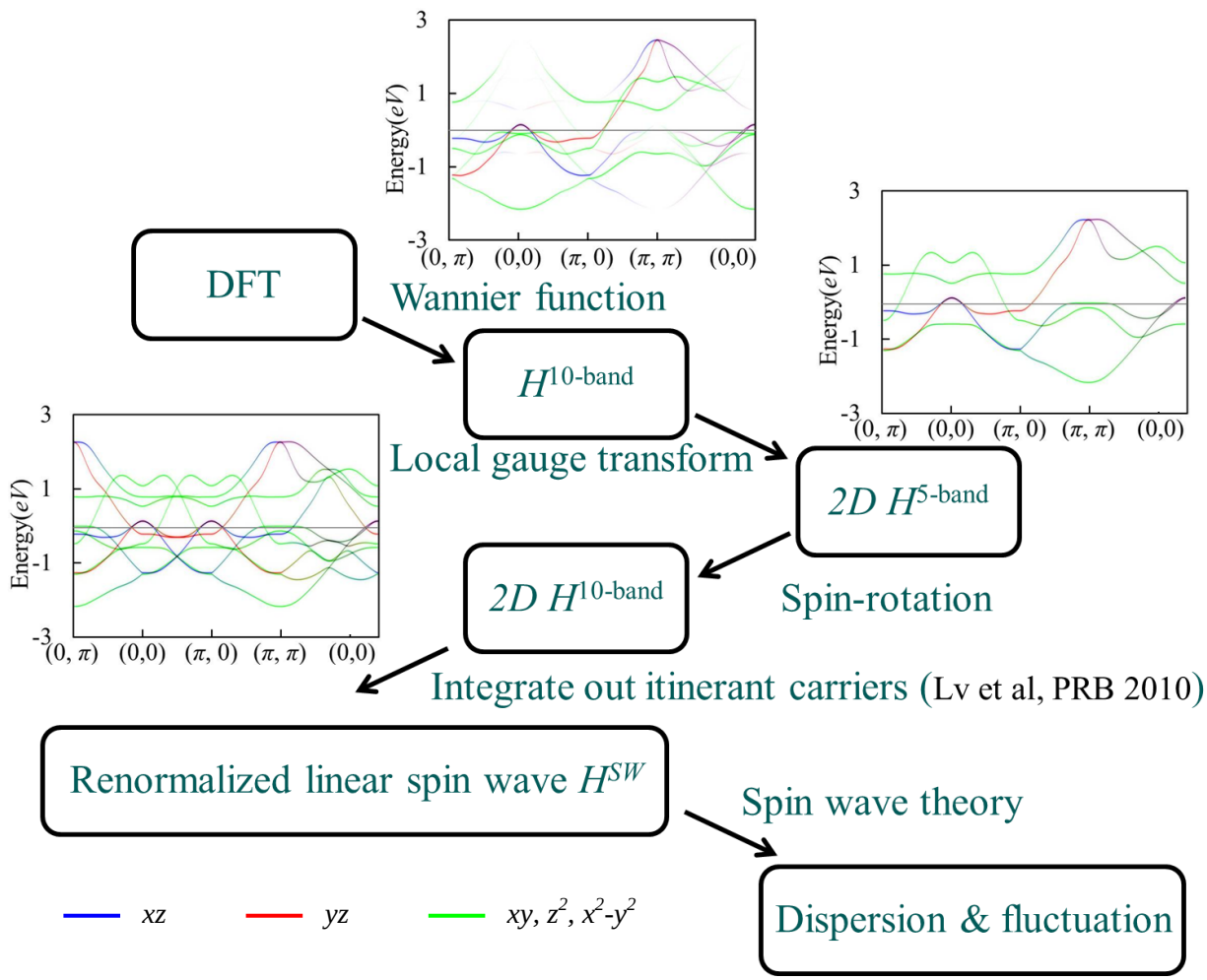

We start with a density functional theory calculation using the experimental lattice constant. We then construct the low-energy Wannier orbitals spanning the energy window of the Fe-*d* bands, and use them to represent the fully self-consistent Kohn-Sham Hamiltonian of the normal state. These steps have been reported previously [C.-C. Lee et al., PRL 103, 267001 (2009)]. The

resulting three-dimensional Hamiltonian contains 10 bands, because there are two Fe atoms in the unit cell due to the alternating tetrahedron positioning of the As atoms around each Fe atom. We then perform the local gauge transformation [Lee and Wen, Phys. Rev. B 78, 144517 (2008)] that changes the sign of the orbitals of even *z*-parity on the even lattice sites, to take into account the glide translational symmetry and recover a nearly translational symmetry Hamiltonian in the new "pseudo-momentum" space. Upon dropping the small out-of-plane terms, we finally obtain a translation symmetric two-dimensional 5-band Hamiltonian for the itinerant carriers. This final Hamiltonian corresponds to one Fe in the unit cell, and is thus consistent with the unit of local moments to be considered in the next step.

II. Integrating out the itinerant carriers

Our goal is to study the influence of the itinerant carriers on dispersion and fluctuation of local moments. We thus follow the procedure reported in [Lv, el al. PRB 82, 045125 (2010)] to integrate out the itinerant carriers to obtain a effective linear spin-wave Hamiltonian. It is convenient to first perform a spin rotation for the site of even columns of sites $S_i^x = \tilde{S}_i^x$, $S_i^y = \kappa_i \tilde{S}_i^y$ and $S_i^z = \kappa_i \tilde{S}_i^z$, where $\kappa_i = \exp(\mathrm{i}\mathbf{Q}\cdot\boldsymbol{r}_i) = \pm 1$, and $\tilde{c}_{i,\uparrow} = c_{i,\downarrow}$, such that in the rotated frame, all the ordered local moments are pointing toward the "up" direction. Note that in this new frame, the itinerant Hamiltonian again resumes a 10-band form, since now spin up and spin down channels couple together after the spin rotation.

We then use the lowest-order Holstein-Primakoff boson: $\tilde{S}_i^z = S - a_i^\dagger a_i$, $\tilde{S}_i^+ = \sqrt{2S} a_i$, $\tilde{S}_i^- = a_i^\dagger \sqrt{2S}$, to capture the bare spin-excitation of the local moment via the spin-wave Hamiltonian (in unit of S^2):

$$\mathcal{H}_{loc} = \sum_q [A_0(q)\left(a_q^\dagger a_q + a_{-q} a_{-q}^\dagger\right) + B_0(q)\left(a_q^\dagger a_{-q}^\dagger + a_{-q}\, a_q\right)] \qquad [1]$$

where,

$$A_0(q) = 2(J_1 cos q_y + 2J_2)/S$$

$$B_0(q) = 2(J_1 cos q_x + 2J_2 cos q_x cos q_y)/S$$

Treating the Hund's coupling between the itinerant and local degrees of freedom, $\frac{J_H}{2S}$, as perturbation

$$\mathcal{H}_H = -\frac{J_H}{2S} \sum_{i,\alpha,\nu\nu'} \boldsymbol{S}_i c_{i\alpha\nu}^\dagger \boldsymbol{\sigma}_{\nu\nu'} c_{i\alpha\nu'} \qquad [2]$$

where $\boldsymbol{\sigma}_{\nu\nu'} = (\boldsymbol{\sigma^x}, \boldsymbol{\sigma^y}, \boldsymbol{\sigma^z})_{\nu\nu'}$ with $\boldsymbol{\sigma^\alpha}$, the canonically transformed full Hamiltonian (Eq.1 of the manuscript)

$$e^{\Delta}\mathcal{H}e^{-\Delta} = \mathcal{H} + [\Delta, \mathcal{H}] + \frac{1}{2}\big[\Delta, [\Delta, \mathcal{H}]\big] + \cdots \quad [3]$$

gives the renormalized linear spin-wave Hamiltonian from its quadratic components:

$$\mathcal{H}^{sw} = \mathcal{H}_{loc}^{sw} + \langle \mathcal{H}_H^2 + \frac{1}{2}\left[\Delta, \mathcal{H}_H^{(1)}\right]\rangle_e = \sum_q [A(q)\big(a_q^\dagger a_q + a_{-q}a_{-q}^\dagger\big) + B(q)\big(a_q^\dagger a_{-q}^\dagger + a_{-q}\, a_q\big)] \quad [4]$$

up to 2nd order in 1/S, where

$$A(q) = A_0(q) + A_1 + A_2(q) \quad [5]$$

$$B(q) = B_0(q) + B_2(q) \quad [6]$$

$$A_1 = \frac{J_H}{2S}\sum_{k,n} f_n(k) \sum_{\alpha,\upsilon} \upsilon |U_{\alpha\nu}^n(k)|^2 \quad [7]$$

$$A_2(q) = \frac{{J_H}^2}{2S}\sum_{k,mn} \frac{f_n(k) - f_m(k+q)}{E_n(k) - E_m(k+q)} |\sum_\alpha U_{\alpha\downarrow}^{m*}(k+q) U_{\alpha\uparrow}^n(k)|^2 \quad [8]$$

$$B_2(q) = \frac{{J_H}^2}{2S}\sum_{k,mn} \frac{f_n(k) - f_m(k+q)}{E_n(k) - E_m(k+q)} \times \sum_{\alpha\beta} U_{\alpha\downarrow}^{m*}(k+q) U_{\alpha\uparrow}^n(k) U_{\beta\downarrow}^{n*}(k+q) U_{\beta\uparrow}^m(k) \quad [9]$$

Here diagonal representation d_{nk} of the itinerant Hamiltonian (including the influence of ferro-orbital and anti-ferromagnetic order parameters) is employed $\tilde{c}_{k\alpha\nu} = \sum_n U_{\alpha\nu}^n(k) d_{nk}$, with eigenvalue $E_n(k)$ of each band index n. Note that $f_n(k) = 1/(1 + e^{\beta(E_n(k) - \mu)})$ denotes the Fermi distribution function with chemical potential μ., which needs to be evaluated for each set of order parameters.

Finally, a simple diagonalization of the spin-wave Hamiltonian gives the spin-wave dispersion

$$\omega(q) = \sqrt{A^2(q) - B^2(q)} \quad [10]$$

and allows an estimation of the fluctuating portion of the moment

$$\Delta m = \frac{1}{8\pi^2}\int dq^2 A(q)/\omega(q) - 1/2 = \frac{1}{8\pi^2}\int dq^2 [1 - (B_q/A_q)^2]^{-1/2} - 1/2 \quad [11]$$

III. Some useful numerical tricks

q-space interpolation

Since the formula to evaluate Δm involves integrable singularity, an accurate and very dense mesh of q points is necessary. Making use of the smooth nature of A_q and B_q, a useful trick is to evaluate q only in a relatively coarser mesh, say 20×20 or bigger, and then perform Wannier interpolation to generate a denser mesh, say 20000×20000 for the computation of Δm. The simple idea of Wannier interpolation is to Fourier transform A_q and B_q to real space, and enlarges

the size of the periodic boundary condition by filling zeros in the long-range tail, and inverse Fourier transform back to q space. The smoothness of A_q and B_q guarantees the smallness of long-range tail and makes this trick an accurate numerical approximation.

Special treatment near zero energy when evaluating Δm

In evaluating Δm , one needs to perform the following integration

$$\frac{S}{8\pi^2}\int dq^2 SA(q)/\omega(q) \qquad [12]$$

Therefore, special treatment in region of q where the spin wave energy become close to zero. A useful simple trick is to reduce the integration to one-dimension and use semi-analytical approach to treat the small energy region.

$$\frac{S}{8\pi^2}\int dq^2 A(q)/\omega(q) = \int dv\, g^A(v)/v \qquad [13]$$

where

$$g^A(v) = \frac{S}{8\pi^2}\int dq^2 A(q)\delta\big(v-\omega(q)\big) \qquad [14]$$

is the *A*-weighted density of states. One thus can take the linear coefficient of the expansion of g^A and perform the integration analytically within a small energy range. Caution must be paid though, when the system is close to a phase transition and the linear region of g^A becomes small in energy.

IV. Band structure and Fermi surface employed in Ref. 21

The very different physical conclusions between our study and that of Ref.21 originate from the different electronic structure of itinerant carriers. Ref. 21 uses a very low filling factor (~0.1), corresponding to a chemical potential μ ~ -2.31t_1, so that there are only two electron pockets in the center of the Brillouin zone, as shown in the figures below (obtained with the same parameters as those in Ref.21.).

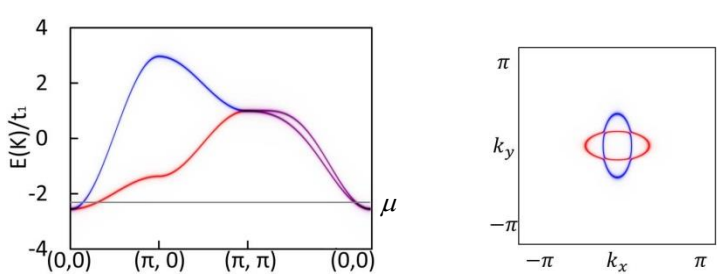

V. Evolution of Fermi surface and band structure via ferro-orbital order and magnetic order

The figures below compare the effects of ferro-orbital and magnetic order on the band structures and Fermi surfaces.

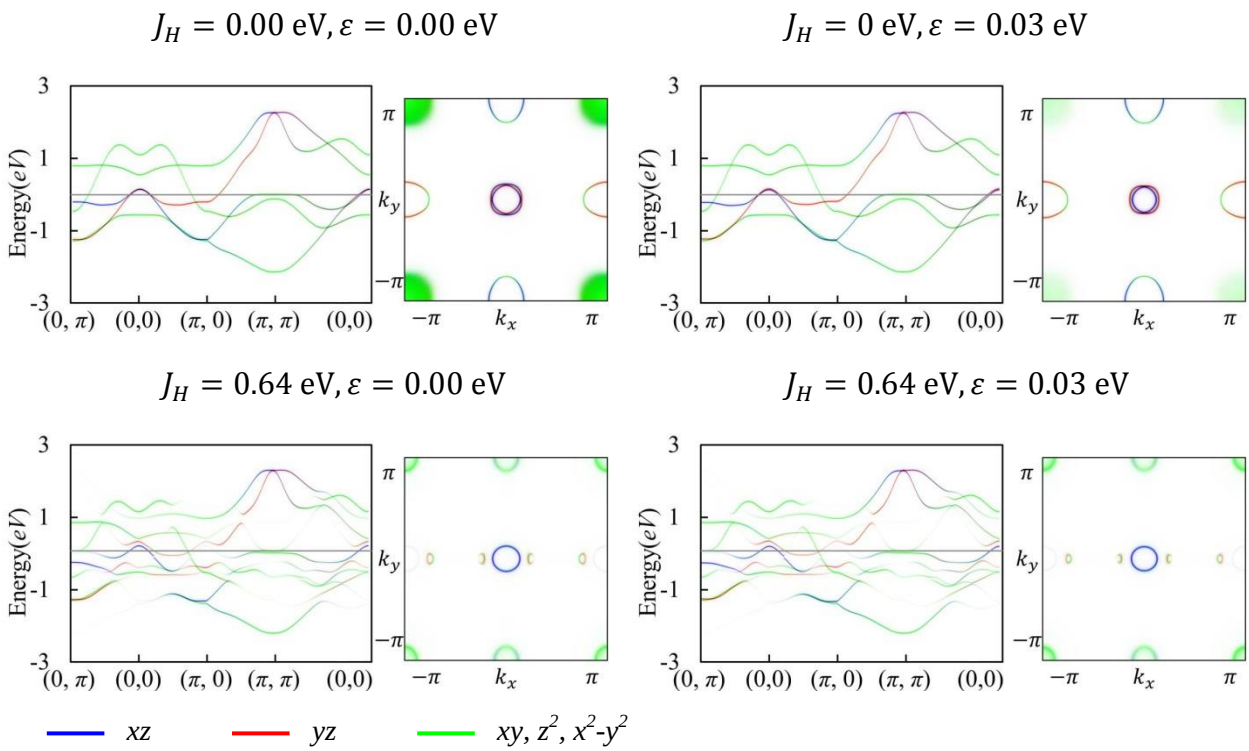

VI. Insensitivity of qualitative trends against the thermal broadening parameter

Our study considers [Eq.(4)] only the zero-temperature quantum fluctuation Δm without thermal fluctuation. The thermal broadening parameter T in the itinerant side is introduced only to ease the numerical calculation. Particularly, we aim at revealing the generic trends in Fe-SCs originated from the approximately nested electron and hole pockets, rather than the material dependence dictated by the details of the Fermi surface. Choosing a larger T thus also helps us avoid being overwhelmed by the details of the Fermi surface of one particular material.

The following figures compare results with two different T parameters (keeping all other parameters identical) and demonstrate clearly the same qualitative trends.

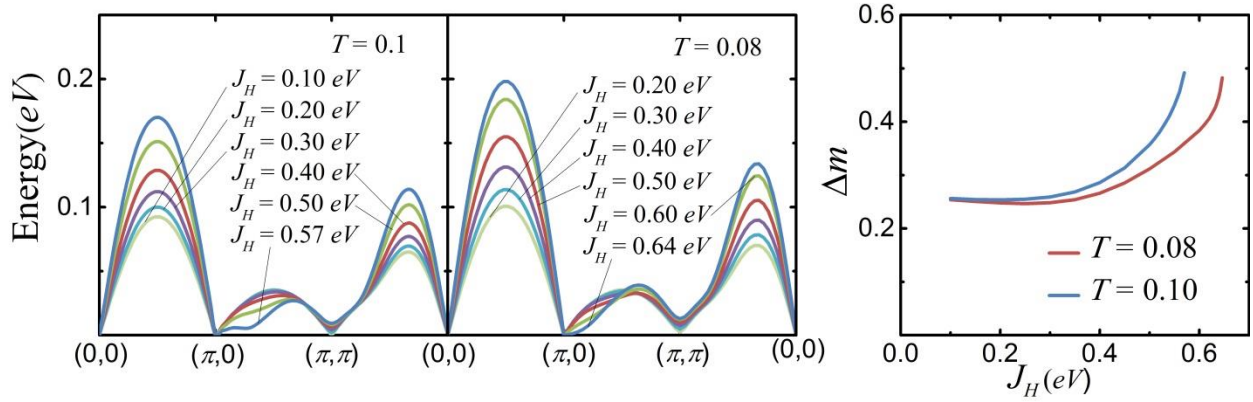

VII. Other physical considerations

We add here some additional physical consideration that may be considered in future investigations. First, our study focuses on the dominant fluctuation of the local moment, in the spin direction. There in principle should also be weaker fluctuation in the amplitude, since this is an itinerant system. From the phase space argument similar to Pauli vs. Curie susceptibility, one of course would expect such amplitude fluctuation be much weaker at low temperature.

Second, from the separation of local and itinerant degrees of freedom, one should expect that the low-energy bands might not have a full spectral weight of one. The reduced spectral weight should then reduce slightly these bands' contribution to the renormalization, in A_1, A_2, and B_2.

Similarly, one should in principle feed the resulting reduced magnetic order parameter back to the itinerant Hamiltonian, in a self-consistent manner. This would stretch the region of fluctuation to a larger region in the phase diagram, making it more similar to the real materials. The qualitative trends illustrated in the manuscript, however, will remain the same. The last two considerations together can be approximately simulated with a smaller value of J_H, as is done in our manuscript.